

Polymer-Supported Photosensitizers for Oxidative Organic Transformations in Flow and Under Visible Light Irradiation

John M. Tobin,[†] Timothy J. D. McCabe,[‡] Andrew W. Prentice,[†] Sarah Holzer,[†] Gareth O.

Lloyd,[†] Martin J. Paterson,[†] Valeria Arrighi,[†] Peter A. G. Cormack^{‡} and Filipe Vilela^{*†}*

[†]School of Engineering and Physical Sciences, Heriot-Watt University, Edinburgh, EH14 4AS, Scotland, United Kingdom.

[‡]WestCHEM, Department of Pure and Applied Chemistry, University of Strathclyde, Thomas Graham Building, 295 Cathedral Street, Glasgow, G1 1XL, Scotland, United Kingdom.

ABSTRACT. A 2,1,3-benzothiadiazole (BTZ)-based vinyl crosslinker was synthesized and copolymerized with large excesses of styrene using free radical polymerization to deliver heterogeneous triplet photosensitizers in three distinct physical formats: gels, beads and monoliths. These photosensitizers were employed for the production of singlet oxygen ($^1\text{O}_2$) and for the aerobic hydroxylation of aryl boronic acids *via* superoxide radical anion ($\text{O}_2^{\cdot-}$) whereby the materials demonstrated good chemical and photo stability. BTZ-containing beads and monoliths were exploited as photosensitizers in a commercial flow reactor, and $^1\text{O}_2$ production

1
2
3 was also demonstrated using direct sunlight irradiation, with a conversion rate comparable to the
4 rates achieved when using a 420 nm LED module as the source of photons.
5
6
7

8
9
10 **Keywords:** *flow chemistry, free-radical polymerization, heterogeneous photosensitizer, reactive*
11 *oxygen species, singlet oxygen, visible light*
12
13

14 15 INTRODUCTION

16
17
18 New advances in photocatalytic processes (including new photocatalysts) have been made in
19 recent years, not only in the production of energy dense materials, as shown in the field of Solar
20 Fuels (with extensive studies on achieving water-splitting and CO₂ reduction), but also in organic
21 synthesis.¹⁻³ These efforts represent a true advancement in realizing more sustainable,
22 economical and environmentally friendly strategies for a wide-range of chemical processes.
23
24
25
26
27
28
29

30 One photocatalytic process that has been under scrutiny is the generation of singlet oxygen
31 (¹O₂) through well-known photosensitization reactions.^{4, 5} These reactions proceed under mild
32 conditions, requiring only a photosensitizer, a light source and molecular oxygen. Organic dyes
33 such as Rose Bengal, Eosin Blue and Methylene Blue, among others, are some of the most
34 commonly used photosensitizers in this process.⁶⁻¹¹ When irradiated with light of an appropriate
35 wavelength, energy is absorbed by the photosensitizer which is excited electronically to the
36 triplet state through an intersystem crossing mechanism. The excited photosensitizer then
37 transfers this energy to the ground state triplet oxygen (³O₂), resulting in the formation of ¹O₂.⁷
38 The electrophilic and oxidizing properties of ¹O₂ have driven its use as an oxidant and as a
39 synthetic reagent in a wide range of applications, such as organic synthesis,¹² water and
40 wastewater treatment¹³ and photodynamic therapy for the treatment of cancer.^{14, 15}
41
42
43
44
45
46
47
48
49
50
51
52
53
54
55
56
57
58
59
60

1
2
3 Another area of catalysis that has come to prominence recently is that of photoredox reactions
4 for organic synthesis.¹⁶ Along with the generation of ¹O₂, photooxidations use molecular oxygen
5 in air as a green reagent, resulting in highly desirable reaction conditions. However, the reactive
6 species for these reactions involve a superoxide radical anion (O₂^{•-}), not the aforementioned ¹O₂.
7 Formation of O₂^{•-} can proceed through a photoredox cycle in the presence of an amine base
8 acting as a sacrificial reductant, a photosensitizer capable of occupying the excited triplet state
9 and molecular oxygen.¹⁷

10
11
12 While both reactive forms of molecular oxygen are generally well-known and have their uses
13 in a variety of applications, many of the photocatalytic materials used rely largely on transition
14 metal complexes or organic dyes, which can lead to several issues. For example, the use of
15 organometallic photosensitizers, while efficient light harvesters,¹⁷⁻²¹ tend to be expensive,
16 unsustainable and toxic. Some photosensitizers are also prone to photobleaching, *i.e.*, the
17 degradation of the photosensitizer due to prolonged exposure to light and/or reactivity with ¹O₂.⁷
18 This leads to both a reduction in the efficiency and the lifetime of the photosensitizer. Lastly,
19 most of these materials are employed under homogeneous conditions, leading to a cumbersome
20 separation and recovery process of the photosensitizer from the reaction mixture, and ultimately
21 the desired products, which impedes the reusability of the photosensitizer.²² These disadvantages
22 demonstrate the need to develop metal-free and photostable materials that can act as
23 heterogeneous photosensitizers in a variety of reactions and conditions.

24
25 In principle, the use of heterogeneous photosensitizers offers advantages in practical
26 applications when compared to their homogeneous counterparts because they are easy to isolate,
27 recover and recycle. Immobilization of commonly used homogeneous photosensitizers, such as
28 organic dyes^{23, 24} and transition metal complexes,²⁵ in polymer matrices has been shown to
29
30
31
32
33
34
35
36
37
38
39
40
41
42
43
44
45
46
47
48
49
50
51
52
53
54
55
56
57
58
59
60

1
2
3 provide a more photostable material. This is due to the polymer matrix acting as an efficient
4 oxygen diffusion barrier whilst inhibiting photobleaching of the photosensitizer.²⁶ However, this
5 immobilization technique may lead to a decrease in the quantum yield of $^1\text{O}_2$ production and
6 therefore its efficiency as a photosensitizer.⁷ Nevertheless, the added benefits of a heterogeneous
7 photosensitizer (ease of recovery, reusability and avoiding contamination of the product)
8 outweigh the lower efficiency of the photocatalytic material.
9

10
11 Recently, we reported the use of conjugated microporous polymers (CMPs) as heterogeneous
12 triplet photosensitizers. Through visible light irradiation, these 2,1,3-benzothiadiazole (BTZ)²⁷⁻²⁹
13 or 4,4-difluoro-4-bora-3a,4a-diaza-s-indacene (BODIPY)-rich³⁰ CMPs have been shown to be
14 efficient and reusable materials for the production of $^1\text{O}_2$. Reports employing heterogeneous
15 photocatalysts for photoredox reactions have begun to emerge, primarily through the use of
16 CMPs.³¹ However, along with this work, CMP synthetic strategies largely involve Pd catalysts,
17 resulting in an expensive material that is likely to be contaminated with residual Pd. Residual
18 metal, even at ppb levels, is problematic as it may interfere with catalytic processes or lead to the
19 toxicity of the reaction medium due to leaching. To circumvent this issue, we have developed a
20 photoactive vinyl monomer, based upon the photoactive repeat unit used within the BTZ-
21 CMPs,²⁷⁻²⁹ which can be incorporated with ease into polymer matrices *via* free radical
22 copolymerization. The BTZ-based monomer contains two styrene units, which results in an
23 electronic “push-pull” system, in which the BTZ unit acts as the strong electron acceptor and the
24 styrene as a weak electron donor. Similarly to the CMPs, we expected that this system would
25 allow the monomer, and polymers derived from the monomer, to act as photosensitizers for the
26 production of $^1\text{O}_2$.
27
28
29
30
31
32
33
34
35
36
37
38
39
40
41
42
43
44
45
46
47
48
49
50
51
52
53
54
55
56
57
58
59
60

1
2
3 One of the most widely available monomers for the production of polymers is styrene, with
4 over 25 million tons produced globally every year.³² It is a highly versatile monomer used to
5 prepare a variety of polymer architectures including linear, branched and crosslinked polymers.
6
7
8 Various formats of polystyrene have been described, such as foams, gels, beads and monolithic
9
10
11
12 structures.³³

13
14
15 Herein, the synthesis and characterization of a photosensitizing crosslinking monomer and its
16
17
18 incorporation into polystyrene structures through free radical copolymerization is presented. A
19
20
21 BTZ-based crosslinker was designed with two styrene units (Scheme 1) allowing for its
22
23
24 exploitation as a co-monomer together with styrene and/or divinylbenzene (DVB) in traditional,
25
26
27 as well as more specialized, free radical polymerization techniques. Using 3-5 mol % only of the
28
29
30 BTZ-based crosslinker, three insoluble forms of photoactive polystyrene were synthesized: gels,
31
32
33 micrometer-sized polymer beads and monoliths. Computational models of the monomer and
34
35
36 polymer repeat unit were investigated to demonstrate their ability to occupy the triplet excited
37
38
39 state and thereby act as triplet photosensitizers. To validate these models, both the monomer and
40
41
42 corresponding polymers were evaluated for the production of $^1\text{O}_2$ in chloroform under both batch
43
44
45 and flow conditions under visible light irradiation (420 nm). Furthermore, the same materials
46
47
48 were screened as triplet photosensitizers in aerobic hydroxylation of a series of aryl boronic acids
49
50
51 *via* the formation $\text{O}_2^{\cdot-}$. These materials have been presented as a proof of concept where both
52
53
54 computational and catalytic experiments verify them as efficient and stable triplet
55
56
57 photosensitizers.
58
59
60

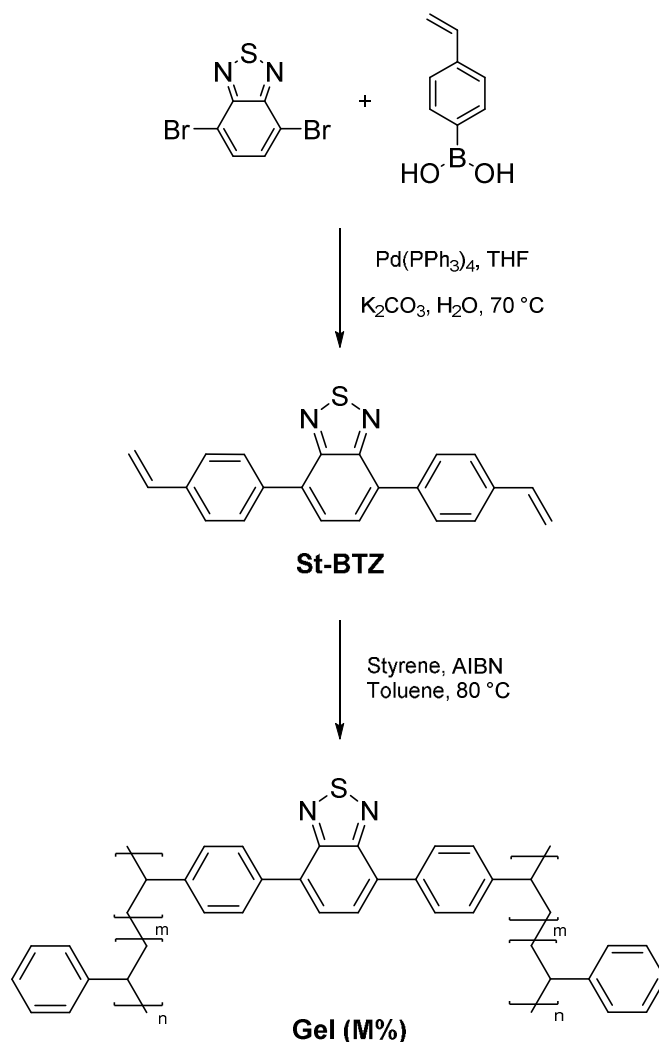
54 **EXPERIMENTAL**

1
2
3
4
5
6
7
8
9
10
11
12
13
14
15
16
17
18
19
20
21
22
23
24
25
26
27
28
29
30
31
32
33
34
35
36
37
38
39
40
41
42
43
44
45
46
47
48
49
50
51
52
53
54
55
56
57
58
59
60

General polymer synthesis and photocatalytic procedures will be described henceforth. All other information pertaining to specific experimental methods not presented here can be found in the ESI.

Synthesis of 4,7-distyrene-2,1,3-benzothiadiazole (St-BTZ). To a dry, 2-necked flask equipped with a magnetic stirring bar and a reflux condenser was added a mixture of 4,7-dibromo-2,1,3-benzothiadiazole (147 mg, 0.5 mmol), 4-vinylphenylboronic acid (148 mg, 1 mmol), and Pd(PPh₃)₄ (17 mg, 0.015 mmol). The flask was connected to a Schlenk line, evacuated and back-filled three times with N₂. In the flask whilst under N₂, dry THF (40 mL) was added to dissolve the solid reagents. An aqueous solution (5 mL) was then prepared with K₂CO₃ (140 mg, 1 mmol), degassed for approximately 10 minutes with N₂ and added to the organic solution. The mixture

Scheme 1. Reaction schemes for the synthesis of the monomer (St-BTZ) and gel-type polymers (Gel (M%)).



was heated to 70 °C and left overnight, stirring under a N₂ atmosphere. The reaction mixture was allowed to cool to room temperature before adding approximately 40 mL of water and transferring to a separating funnel with 50 mL of dichloromethane. The organic layer was washed three times with deionized water and the collected fractions were dried over Na₂SO₄. The crude mixture was filtered and purified *via* silica gel column chromatography with hexane:CH₂Cl₂ (4:6) as eluent, yielding a bright yellow colored solid (96 mg, 56%). ¹H NMR (300 MHz, CDCl₃): δ_{ppm} = 5.36 (d, 1 H), 5.89 (d, 1 H), 6.85 (m, 1 H), 7.63 (d, 2 H), 7.83 (s, 1 H), 8.00 (d, 2 H); ¹³C NMR (100 MHz, CDCl₃): δ_{ppm} = 114.5, 126.5, 127.6, 129.4, 133.0, 136.4, 136.8, 137.7, 154.1.

1
2
3
4
5
6
7
8
9
10
11
12
13
14
15
16
17
18
19
20
21
22
23
24
25
26
27
28
29
30
31
32
33
34
35
36
37
38
39
40
41
42
43
44
45
46
47
48
49
50
51
52
53
54
55
56
57
58
59
60

General synthesis of Styrene-St-BTZ copolymers via free radical polymerization (Gel (M%)). Styrene (1 g, 9.6 mmol) was added to a sample vial with a magnetic stirring bar and dissolved in 5 mL of degassed toluene. **St-BTZ** (2, 3 or 5 mol %) and AIBN (16 mg, 0.096 mmol) were added to the solution, allowed to dissolve and degassed with N₂ for 10 minutes. The vial was sealed, heated to 60 °C and left for 16 h to polymerize while stirring. The solution began as a bright, yellow liquid and changed according to the percentage of **St-BTZ** added. The reaction was allowed to cool to room temperature and the product was removed from the vial and worked up as follows: (i) Precipitation of product was performed in 100 mL of MeOH, for soluble copolymers; (ii) Soxhlet extraction was performed for insoluble (crosslinked) copolymers with THF and methanol. All copolymers were dried *in vacuo*. It is noted that only those polymers containing 3 or more mol % of the **St-BTZ** crosslinker produced an insoluble gel. At concentrations lower than 3 mol % a soluble polymer was formed. Product recovery: **Gel (2%)** 367 mg, 37 %; **Gel (3%)** 240 mg, 24 %; **Gel (5%)** 465 mg, 47 %.

Synthesis of Styrene-DVB-St-BTZ copolymer via precipitation polymerization (Bead-BTZ). DVB-55 (221 mg, 1.7 mmol), styrene (666 mg, 6.4 mmol), **St-BTZ** (115 mg, 0.3 mmol) (2% w/v total monomer in feed, relative to solvent) and AIBN (41 mg, 0.2 mmol) (2 mol % relative to polymerizable double bonds in monomers) were added to acetonitrile (50 mL) in a Nalgene[®] bottle (250 mL). Note that the monomer mole ratio employed for this synthesis was 76:20:4 (styrene:DVB-55:**St-BTZ**), providing a good comparative analogue to the gels. The bottle contents were ultrasonicated for 15 minutes. After ultrasonication, N₂ gas was bubbled through the reaction mixture for 15 minutes in an ice-bath. After degassing, the Nalgene[®] bottle was sealed under N₂ and placed on a low profile roller (Stovall Life Sciences Inc., North Carolina, U.S.A) contained within an incubator (Stuart Scientific, Stone, UK) and rotated slowly

1
2
3 about its long axis. The temperature inside the incubator was ramped from ambient temperature
4
5 to 60 °C over a period of around two hours. The polymerization was allowed to proceed for a
6
7 further 46 hours to give a milky suspension of polymer particles. The resulting particles were
8
9 visualized *via* optical microscopy prior to filtration. The product was filtered by vacuum on a
10
11 0.45 μm nylon membrane filter. The particles were then washed with solvent to remove any
12
13 unreacted monomer or initiator (~100 mL of acetonitrile followed by ~100 mL of toluene,
14
15 methanol and finally acetone) before being dried overnight *in vacuo* (60 mbar, 40 °C). Product
16
17 recovery: 120 mg, 12 %.
18
19
20
21

22 **Synthesis of Styrene-DVB-St-BTZ copolymer *via* high internal phase emulsion**
23 **polymerization (pHIPE-BTZ).** Styrene (0.213 g, 2.04 mmol), DVB-80 (40 mg, 0.29 mmol), St-
24
25 **BTZ** (25 mg, 0.07 mmol) and Span 80 (0.054 mL) were added to a sample vial and potassium
26
27 persulfate (18 mg, 0.2 % wt. of water) and sodium chloride (90 mg, 1 % wt. of water) were
28
29 dissolved in water (9 mL) in a separate vial. Note that the monomer mole ratio was 85:12:3
30
31 (styrene:DVB:St-BTZ), providing a good comparative analogue to the gels. The organic phase
32
33 was placed in an electric mixer (Polytron PT 1200 E) and the aqueous solution was added
34
35 slowly. The addition of the aqueous solution was stopped when the emulsion could no longer be
36
37 mixed properly due to thickening. Remaining liquid was decanted and part of the emulsion was
38
39 delivered into a transparent glass column (7 mm inner diameter) equipped with porous frit on
40
41 both ends *via* syringe. The column was sealed and placed in a 60 °C oven and left for 24 h. The
42
43 column containing the synthesized polyHIPE was flushed with 100 mL of THF, CH₂Cl₂ and
44
45 chloroform. The bright yellow monolith (35 mm length x 7 mm diameter) was left in the glass
46
47 column to be used for flow experiments.
48
49
50
51
52
53
54
55
56
57
58
59
60

1
2
3 **Computational modelling of St-BTZ excited states.** Geometry optimization was performed
4 with density functional theory (DFT) using both the CAM-B3LYP and MN12-L functionals,
5 while excited electronic states were computed with time-dependent DFT, utilizing the temporal
6 adiabatic approximation with the same functionals. The 6-311G(d,p) basis set was used for all
7 computations. Analytical Hessian computation was used to confirm optimized stationary
8 geometries as minima. We note only negligible difference between functionals and so discuss the
9 CAM-B3LYP results below (full results for both are given in the supporting information). All
10 computations were performed using Gaussian09.³⁴

11
12 **General procedure for photocatalytic reactions under batch conditions.** To a vial
13 containing the required solution (5-10 mL), 5-10 mg of photosensitizing material was added. The
14 mixture was left to stir, whilst open to air, for 10 minutes to allow for proper dissolution or
15 swelling and to aerate the solution. The vial was then placed 7 cm from a 420 nm LED lamp and
16 the lamp was switched on. The reaction was monitored *via* TLC and/or ¹H NMR spectroscopy
17 until full consumption of the starting materials was noted, at which time the reaction was stopped
18 and analyzed.

19
20 **General procedure for photocatalytic reactions in flow employing Bead-BTZ.** To a flask
21 containing the required solution (10-15 mL), 5 mg of **Bead-BTZ** was added. The suspension was
22 first sonicated for 2 minutes to ensure an even dispersion of particles. The mixture was then left
23 to stir, whilst open to air, for 10 minutes to aerate the solution. The dispersion was then pumped
24 through the photochemical reactor (Figure S2) at a flow rate of 1 mL.min⁻¹. Concurrently, air
25 was pumped through a second pump at the same flow rate, mixing with the dispersion at a T-
26 junction before entering the photochemical reactor equipped with a 420 nm LED lamp. The
27 dispersion was cycled for the required time and monitored *via* TLC and/or ¹H NMR
28
29
30
31
32
33
34
35
36
37
38
39
40
41
42
43
44
45
46
47
48
49
50
51
52
53
54
55
56
57
58
59
60

1
2
3 spectroscopy. Upon consumption of the starting materials, the reaction was stopped and
4
5 evaluated further.
6

7
8 **General procedure for photocatalytic reactions in flow employing pHIPE-BTZ.** The
9
10 **pHIPE-BTZ** monolith, fitted to a transparent glass column, was allowed to swell in the required
11
12 solvent for 16 hours. The solution containing the starting materials (10 mL) was prepared and
13
14 aerated for 10 minutes open to air. The column was fitted to a light source (Figure S3) and the
15
16 solution was pumped through the column at 0.5-1.0 mL.min⁻¹. Concurrently, oxygen was
17
18 pumped through a second pump at the same flow rate, mixing with the solution at a T-junction
19
20 before entering the column. The operating pressure was kept at 1.3 bar to ensure a steady stream
21
22 of both the solution and air. The 10 mL solution was pumped through the column and monitored
23
24 *via* TLC and/or ¹H NMR spectroscopy. Upon consumption of the starting materials, the reaction
25
26 was stopped and evaluated.
27
28
29
30
31
32
33

34 RESULTS AND DISCUSSION

35
36 **Monomer properties.** The UV-Vis absorption spectra for **St-BTZ** presented as a broad
37
38 absorption peak in the range 350 to 450 nm with a maximum absorbance at 400 nm (Figure S13).
39
40 This falls within the visible spectrum and is comparable to the absorbance characteristics which
41
42 we have reported for other BTZ-based photosensitizers.²⁷⁻²⁹ FT-IR, ¹H NMR and ¹³C NMR
43
44 spectroscopic analysis was fully consistent with the structure of **St-BTZ** (see ESI). An X-ray
45
46 crystal structure and the corresponding analysis data can also be found in the ESI.
47
48
49

50
51 By virtue of its polymerizable vinyl groups, **St-BTZ** can be copolymerized with styrene *via*
52
53 free radical polymerization. Similarly to DVB, **St-BTZ** can act as a branching node and
54
55 consequently as a crosslinker. Employing the crosslinker at an appropriate concentration in a
56
57
58
59
60

1
2
3 copolymerization can result in an insoluble, crosslinked polymer that can then be employed as a
4
5 heterogeneous photosensitizer.
6
7

8 **Synthesis and properties of Gel (M%).** One of the key aims of the work was to minimize the
9 amount of photoactive **St-BTZ** required whilst ensuring the formation of an insoluble polymer
10 with the desired photosensitizing properties. The selection of styrene as co-monomer as the basis
11 for the heterogeneous photosensitizer was influenced by the stability of polystyrene in the
12 presence of $^1\text{O}_2$ ³⁵ and the fact that the photoactive monomer also contains styrene units, which
13 leads to a more compatible copolymerization between the co-monomers.
14
15
16
17
18
19
20
21

22 The formation of these polymers (**Gel (3%)** and **Gel (5%)**) suggests that there was sufficient
23 crosslinking of the polymer chains to create an insoluble material. The bright yellow color,
24 similar to that of **St-BTZ**, is also indicative of the integration of the photoactive crosslinker into
25 the polymer network. Most of the solvent used in these reactions was sorbed by the polymers,
26 resulting in bright yellow, swollen gels (Figure 1). A swelling test was performed on dried **Gel**
27 (**3%**), demonstrating an increase of up to seven times its original volume when added to
28 chloroform (Figure S1).
29
30
31
32
33
34
35
36
37

38 UV-Vis absorption spectra of the materials showed a broad absorption band (350-450 nm)
39 with a maximum at 400 nm (Figure S13). FT-IR spectroscopic measurements showed peaks
40 corresponding to **St-BTZ** residues (825 and 887 cm^{-1}), which were not observed in a polystyrene
41 standard (Figure S12). Note that these signals were relatively weak due to the high ratio of
42 styrene to **St-BTZ** within the polymer.
43
44
45
46
47
48
49
50
51
52
53
54
55
56
57
58
59
60



Figure 1. Inverted reaction vials showing **Gel (3%)** (left) and **Gel (5%)** (right) as insoluble gels swollen in chloroform.

Solid state ^{13}C NMR CP-MAS spectroscopy was also employed to characterize **Gel (3%)**. Whilst aromatic carbons are present primarily, at 128 ppm (C-C) and 146 ppm (C-N), signals in the alkyl region are also identified at 40-45 ppm and correspond to the saturated aliphatic backbone of the copolymer (Figure S18). These observations suggest that **St-BTZ** was incorporated successfully into the polystyrene chains *via* well-established, metal-free, free radical polymerization and that the polymer has the potential to be used a polystyrene-based heterogeneous photosensitizer.

Heterogeneous phase polymerizations (including emulsion, dispersion, precipitation and suspension polymerization)³³ using the same free radical initiator allow us to demonstrate the versatility of the photoactive crosslinker. This versatility arises from the ability of **St-BTZ** to be implemented in a variety of free radical polymerization techniques whilst yielding polymers which retain the photoactive properties of the monomer. For the purposes of this study, precipitation polymerization and high internal phase emulsion (HIPE) polymerization were employed, which allows for the synthesis of the polymers in different physical formats derived from the same monomer set: micron-sized beads from precipitation polymerizations and monolithic structures from HIPE polymerizations.

1
2
3 **Precipitation polymerization (Bead-BTZ).** As seen in Scheme S2, precipitation
4 polymerization utilizing a free radical initiator was used to synthesize particles in the form of
5 micron-sized beads. In order to ensure the production of an insoluble polymer, divinylbenzene-
6 55 (DVB-55) was added as a non-photoactive crosslinker. The incorporation of DVB as a
7 crosslinker also adds rigidity to the structure and good mechanical robustness to the beads. In
8 parallel with the photoactive polymer synthesis, a styrene-DVB copolymer (**Bead**) was
9 synthesized without any photoactive component for comparison.
10
11
12
13
14
15
16
17
18
19

20 UV-Vis spectroscopy showed a maximum absorption at ~420 nm for **Bead-BTZ**, which is
21 comparable to the absorbance wavelength of the previously described materials (Figure S15).
22 **Bead** did not display any absorption in the visible region and produced a white product
23 compared to the bright yellow **Bead-BTZ** material. An FT-IR spectrum of **Bead-BTZ** showed
24 the two distinct peaks characteristic of **St-BTZ** (887 and 825 cm^{-1}). These peaks were not
25 observed for **Bead** (Figure S14). Figures 2a and 2b show both bead types together with the
26 corresponding SEM images. These images show the polymer microspheres very clearly, with a
27 bead size range of approximately 1-2 μm for both materials. While **Bead** resulted in better-
28 defined particles, **Bead-BTZ** showed some signs of aggregation and agglomeration. Based on
29 these observations, we concluded that the **St-BTZ** crosslinker was integrated successfully into
30 the polystyrene beads.
31
32
33
34
35
36
37
38
39
40
41
42
43
44
45

46 **High Internal Phase Emulsion Polymerization (pHIPE-BTZ).** The synthesis of **pHIPE-**
47 **BTZ** was carried out through the free radical polymerization of a high internal phase emulsion
48 (Scheme S3). A UV-Vis spectrum showed a maximum absorption at ~420 nm for **pHIPE-BTZ**,
49 which is comparable to the absorption wavelengths of the other synthesized polymers (Figure
50 S15). An FT-IR spectrum showed only weak bands attributable to **St-BTZ** (887 and 825 cm^{-1})
51
52
53
54
55
56
57
58
59
60

(Figure S14). Figure 2c shows **pHIPE-BTZ** in the column and the corresponding SEM image. This image demonstrates the high degree of porosity typical of polyHIPEs. Again, DVB was a crucial component to stabilize the structure as attempts with only **St-BTZ** (3-5 mol %) as the crosslinker resulted in amorphous, gel-like polymers.

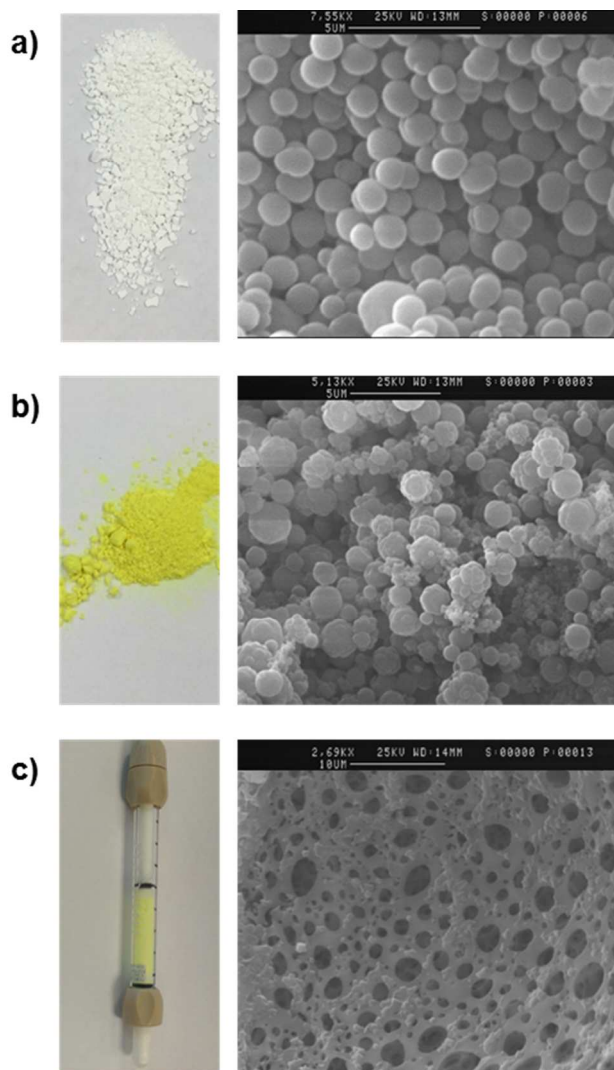


Figure 2. Synthesized copolymers and the corresponding SEM images: a) **Bead** containing no **St-BTZ**; b) **Bead-BTZ** with a yellow color indicating incorporation of **St-BTZ**; c) **pHIPE-BTZ** contained within a column as a stationary material for flow applications.

1
2
3 Given the variety of free-radical polymerization techniques used, the synthesized monomer
4 showed exceptional versatility and stability. By incorporating very limited amounts of the
5 monomer into a polymer matrix, we were able to dilute the amount of photoactive component
6 when compared to more common materials, as previously described. To better understand these
7 materials as potential triplet photosensitizers, computational excited state data were gathered.
8
9

10
11
12
13
14 **St-BTZ excited state computational modelling.** Computations have been performed to
15 investigate the lowest singlet and triplet state geometries, and a characterization of vertical
16 electronic excited states, for the **St-BTZ** monomer and in the absence of vinyl groups as it would
17 appear in the photoactive polymers. For the systems investigated both C_2 and C_s ground state
18 singlet conformers are found (differing in relative sign of dihedral twist for the benzene rings).
19 Each isomer is essentially isoenergetic and results below are for the C_2 matching the crystal
20 structure (further comparison in ESI). We note generally very good agreement for the S_0
21 geometry with experiment. For both systems the lowest singlet and triplet states are of the same
22 character, being 94% represented by the HOMO-LUMO orbital transition (Table S1 and S2).
23 This corresponds to charge transfer through the π -system from the styrene-benzene/isopropyl-
24 benzene groups to the BTZ group as shown in Figure 3 below for the monomer and polymer
25 systems. Finally in Table S3 we give the singlet-triplet energy gap computed at the optimized
26 triplet state geometry for both systems. There is around a 0.8 eV triplet stabilization from the
27 vertical geometry for both systems.
28
29
30
31
32
33
34
35
36
37
38
39
40
41
42
43
44
45
46
47

48 Computational verification of the synthesized materials demonstrated their potential to occupy
49 the triplet excited state. These results showed promise and prompted investigations into their
50 catalytic capabilities. For the purposes of this study, we explored their ability to act as triplet
51 photosensitizers in both the production of 1O_2 and $O_2^{\cdot-}$. Furthermore, due to the photoactive
52
53
54
55
56
57
58
59
60

component being dramatically reduced within the polymeric materials, it was of great interest to understand if this had any significant effect on their ability to act as photosensitizers.

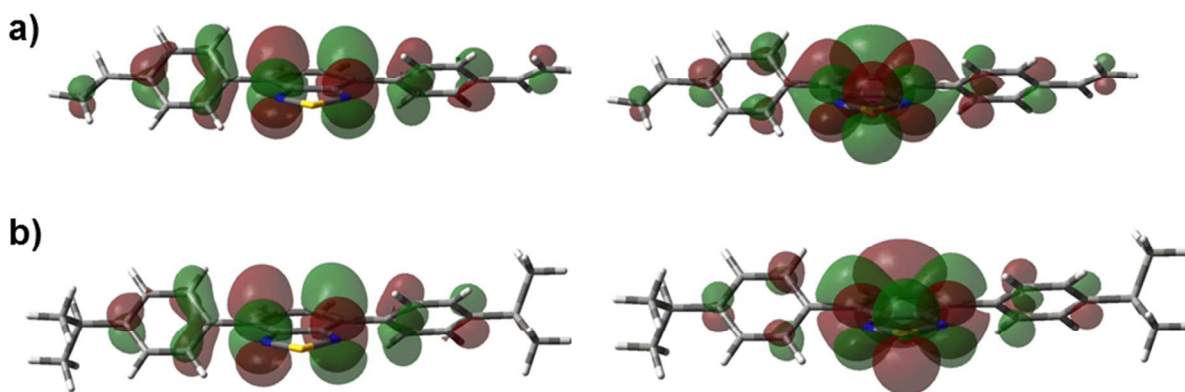
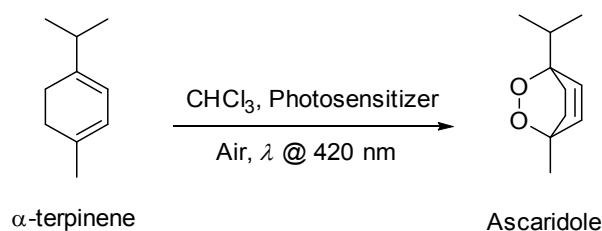


Figure 3. NTO particle-hole representation of a) **St-BTZ** monomer and b) polymer repeat unit T_1 state, computed with TD-CAM-B3LYP/6-311G(d,p).

Homogeneous photosensitization at 420 nm with St-BTZ. The **St-BTZ** crosslinker was first examined as a homogeneous triplet photosensitizer in the production of 1O_2 . Scheme 2 shows the Alder-ene reaction, which only proceeds in the presence of 1O_2 .³⁶ The production of 1O_2 was monitored by observing the conversion of α -terpinene into ascaridole *via* 1H NMR spectroscopy (Figure S20). Full conversion to ascaridole was observed after 90 minutes of irradiation. However, a sudden decrease in the rate of conversion of α -terpinene to ascaridole was observed after 45 minutes, causing near full conversion to take upwards of 90 minutes.

Scheme 2. Synthesis of ascaridole from α -terpinene *via* the photosensitization of singlet oxygen under visible light irradiation.



1
2
3 Samples taken at 15-minute time intervals revealed a dramatic color change (Figure S21),
4 prompting further investigations to determine any potential photo-degradation or oxidative effect
5 on **St-BTZ**. ^1H NMR spectroscopic analysis for each sample confirmed the degradation of the
6 photosensitizer, where a clear decrease in the characteristic peaks for the monomer was observed
7 (Figure S20).
8
9

10
11
12
13
14
15 Unsurprisingly, interactions between $^1\text{O}_2$ and vinylarenes can result in the production of
16 monoadducts and endoperoxides.³⁷ The reaction potential of the vinyl groups may also have
17 increased due to the electron withdrawing effects of the BTZ component within the monomer.
18
19
20
21
22 Along with the known reactivity between vinylarenes and $^1\text{O}_2$, these observations demonstrate
23 the instability of **St-BTZ** under highly oxidative conditions. Degradation issues aside, we were
24 able to demonstrate the ability of **St-BTZ** to act as a triplet photosensitizer in the production of
25 $^1\text{O}_2$ under visible light irradiation. However, we have shown in the past that when incorporating
26 BTZ-based building blocks into CMPs, the stability of the resulting CMP upon production of $^1\text{O}_2$
27 is increased when compared to the monomeric version of BTZ.²⁷⁻²⁹ Therefore, and knowing that
28 polystyrene is largely unaffected by $^1\text{O}_2$,³⁵ we postulated that incorporating **St-BTZ** into a
29 polystyrene matrix would mitigate the photo-degradation or oxidative effect on the polymer.
30
31
32
33
34
35
36
37
38
39
40

41 **Heterogeneous photosensitization at 420 nm with Gel (M%).** A procedure similar to that
42 described above for **St-BTZ** (Scheme 2) was employed with a reaction time of 60 minutes. Three
43 control experiments were performed first, as follows: (i) in the absence of any photosensitizing
44 material; (ii) using a polystyrene standard as the photosensitizer; (iii) performing the experiment
45 in the dark and in the presence of **Gel (3%)**. Each of these controls showed no conversion of α -
46 terpinene to ascaridole, and therefore that $^1\text{O}_2$ was not produced under these conditions.
47
48
49
50
51
52
53
54
55
56
57
58
59
60

As seen in Figure 4, both **Gel (3%)** and **Gel (5%)** showed comparable conversion rates, with close to full conversion achievable after 60 minutes of irradiation. Interestingly, compared to these heterogeneous photosensitization experiments, both homogeneous analogues, **St-BTZ** and **Gel (2%)**, gave significantly reduced conversion rates. The reduction in the rate of $^1\text{O}_2$ production with **Gel (2%)** can be explained by a decrease in the level of the photoactive monomer within the material. As the photoactive **St-BTZ** content decreases, there are fewer accessible sites for an energy transfer to $^3\text{O}_2$, resulting in reduced production of $^1\text{O}_2$. The reduced rate of $^1\text{O}_2$ production with **St-BTZ** has been explored as explained above. ^1H NMR spectra corresponding to each reaction can be found in the ESI.

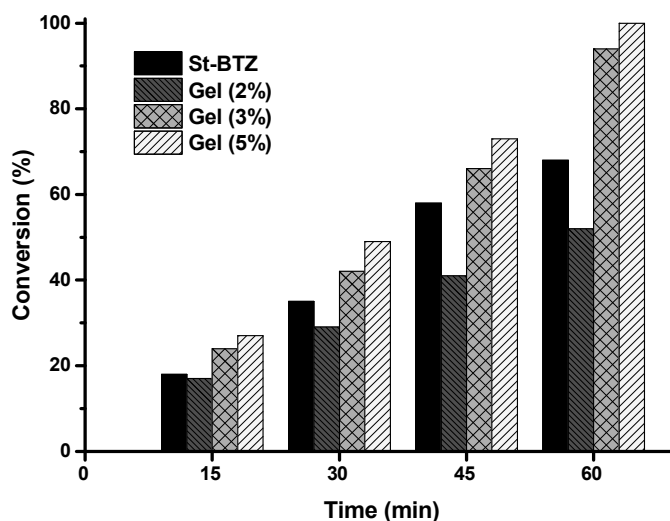


Figure 4. Conversion rates of α -terpinene to ascaridole using $^1\text{O}_2$ produced from the irradiation of **St-BTZ**, **Gel (2%)**, **Gel (3%)**, and **Gel (5%)** with a 420 nm LED lamp.

Based on these results, it is clear that the insoluble photoactive gels performed more efficiently than their soluble counterparts. While **Gel (5%)** performed slightly better than **Gel (3%)**, it also required a greater amount of the photoactive monomer. The gels also displayed greater stability

1
2
3 than **St-BTZ**; no appreciable color change was observed over the reaction period. Most notably,
4
5 these results demonstrate the generation of $^1\text{O}_2$ with a heterogeneous photosensitizer where the
6
7 main component is polystyrene (95-97%). This is advantageous and cost-effective since it
8
9 reduces the amount of **St-BTZ** required in the copolymer to produce $^1\text{O}_2$ when compared to
10
11 other heterogeneous photosensitizers where each repeat unit consist of a BTZ monomer.^{7, 27-29}
12
13 Moreover, self-quenching of the desired triplet state between photocatalytic segments of the
14
15 polymer can occur if the concentration of the photoactive component is too great. This can
16
17 greatly hinder the triplet state lifetime, and therefore diminish the effectiveness of the material as
18
19 a photosensitizer. By reducing the concentration of **St-BTZ** the self-quenching effect is
20
21 mitigated greatly without compromising the ability of the polymers to act as photocatalysts.⁸
22
23 These concepts are crucial when investigating routes to both reduce the cost and increase the
24
25 sustainability and effectiveness of photoactive materials.
26
27
28
29
30

31
32 **Application of Bead-BTZ and pHIPE-BTZ in continuous flow.** Continuous flow chemistry,
33
34 as an alternative to standard batch synthesis, offers a flexible route to photochemical reactions,
35
36 particularly when approaching industrial scales.³⁸ Reactions using this method allow for
37
38 streamlined and continuous production of materials along with the potential for work-up and
39
40 analysis integration.³⁹ This is critically important within industrial processes as it has the
41
42 potential to both reduce costs and increase productivity. This is especially true for photochemical
43
44 transformations as the irradiation of light to a solution is more efficient due to the shorter path
45
46 lengths when compared to traditional batch processes. On larger industrial scales, photon
47
48 penetration depth and excessive irradiation can be problematic under traditional batch
49
50 conditions.⁴⁰ Continuous flow addresses these issues through higher surface-to-volume ratios and
51
52 more efficient heat transfer. This allows for investigations into new synthetic pathways and
53
54
55
56
57
58
59
60

1
2
3 reaction methodologies.⁴¹ Photochemical reactions have been demonstrated widely using
4
5 continuous flow methods, even under heterogeneous conditions.^{29, 41}
6
7

8 While the synthesized gels showed good $^1\text{O}_2$ production, post-reaction recovery and
9
10 continuous flow chemistry was impractical. When attempted in flow, the gel particles aggregated
11
12 and coagulated within the tubing. For this reason, **Bead-BTZ** and **pHIPE-BTZ** were designed
13
14 specifically for two distinct continuous flow applications: (i) The polymer beads present a
15
16 spherical shape and a low mean particle diameter (1-2 μm), which allows for facile dispersion
17
18 throughout a solvent and low susceptibility to aggregation. These properties allow a dispersion of
19
20 beads within the reaction mixture to flow through a photochemical reactor with greater ease than
21
22 amorphous gels. This dispersion can be recirculated through the flow reactor for the time
23
24 required to complete the reaction; (ii) Unlike the beads, a polyHIPE remains as a stationary
25
26 photosensitizer within a glass column where the reagents flow through the porous structure
27
28 whilst being irradiated by an external light source. This results in the continuous production of
29
30 the target product as long as the polyHIPE remains photoactive.
31
32
33
34
35

36
37 **Heterogeneous photosensitization at 420 nm with Bead-BTZ and pHIPE-BTZ in a**
38
39 **commercial flow reactor.** The freely dispersible beads were investigated both in batch as well
40
41 as under flow conditions. A batch experiment was set up identical to that of **Gel (3%)** to
42
43 compare the production of $^1\text{O}_2$. ^1H NMR spectroscopy revealed similar conversion rates of α -
44
45 terpinene to ascaridole compared to that of **Gel (3%)** (>95%) (Figure S25). This confirmed the
46
47 photosensitizing nature of **Bead-BTZ** and showed no appreciable negative effects due to the
48
49 added DVB-55.
50
51
52

53 A continuous flow experiment was then carried out with **Bead-BTZ** with the experimental set
54
55 up depicted in Figure 5a. The dispersion was recirculated through the photochemical reactor for
56
57
58
59
60

60 minutes where full conversion to ascaridole was observed *via* ^1H NMR spectroscopy (Figure S26). The production rate for the conversion of α -terpinene to ascaridole was found to be 136 $\text{mg}\cdot\text{h}^{-1}$. In order to relate this to the amount of photoactive component in the beads, the production rate of ascaridole per mg of **St-BTZ** in **Bead-BTZ** needs to be evaluated. This corresponds to 680 $\text{mg}\cdot\text{h}^{-1}$.

pHIPE-BTZ was also employed as a photosensitizer under continuous flow conditions. However, the photochemical reactor was replaced with the column containing the trapped photoactive polyHIPE, as described above (Figure 2b). Due to the reduced contact time with **pHIPE-BTZ**, some experimental conditions had to be changed: (i) The concentration of the solution was lowered to 0.4 mmol α -terpinene in 10 mL of chloroform; (ii) air was replaced with pure oxygen; (iii) flow rates of both the reaction mixture and oxygen were reduced to 0.5 $\text{mL}\cdot\text{min}^{-1}$ (Figure 5b). Similarly to the gels, **pHIPE-BTZ** did swell in chloroform. Therefore, the polyHIPE samples were allowed to swell for 16 h in chloroform prior to the introduction of a reaction mixture. These changes were made to allow for a greater opportunity to yield full conversion to ascaridole after a single pass through the irradiated **pHIPE-BTZ** column.

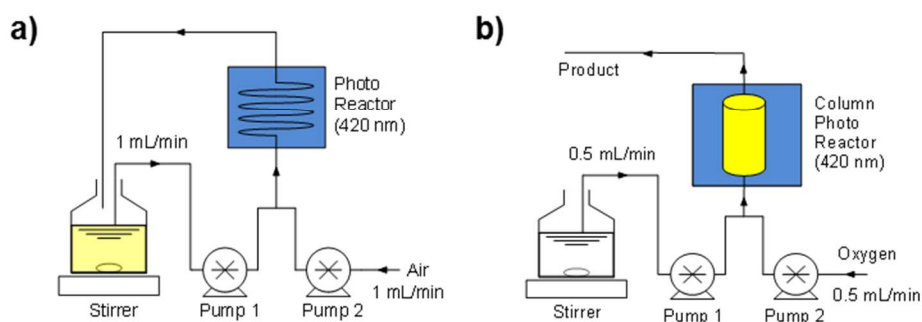


Figure 5. Schematic representation of the experimental set-up using the easy-Photochem flow reactor from Vapourtec Ltd. for a) **Bead-BTZ** and b) **pHIPE-BTZ**.

1
2
3 Under the stated conditions, we observed full conversion of α -terpinene to ascaridole after a
4 single pass of the 10 mL solution of α -terpinene (0.4 mmol in chloroform) (Figure S27). To
5 investigate the reusability of **pHIPE-BTZ**, a continuous stream of the reaction mixture was
6 allowed to flow through the column, taking measurements in 10 mL increments. After 30
7 measurements under continuous flow and irradiation, no decrease in the conversion rate was
8 observed (Figure S28). This suggests that the **pHIPE-BTZ** photosensitizer is stable to both light
9 and $^1\text{O}_2$ over extended usage periods. Moreover, we note that the same column was employed in
10 the photosensitization of $\text{O}_2^{\cdot-}$ for the aerobic hydroxylation of aryl boronic acids (as described
11 below), demonstrating the superior stability of **pHIPE-BTZ** and its potential as a reusable
12 photoactive material.
13
14
15
16
17
18
19
20
21
22
23
24
25

26
27 The production rate for the conversion of α -terpinene to ascaridole under **pHIPE-BTZ**
28 conditions was found to be $192 \text{ mg}\cdot\text{h}^{-1}$. Thus, both of the continuous flow methods provide
29 specific benefits. The use of **Bead-BTZ** in flow results in good production rates where larger
30 quantities of material are required. However, the use of **pHIPE-BTZ** comprises a method in
31 which no intervention is required to obtain the desired product, such as recovery of the polymer
32 from the reaction mixture. These results demonstrate the potential of these stable and reusable
33 materials in heterogeneous photocatalytic applications.
34
35
36
37
38
39
40
41
42

43 **Production of $^1\text{O}_2$ through photosensitization reactions under sunlight irradiation.** To
44 demonstrate further the potential and robustness of these new polymers, a $^1\text{O}_2$ production
45 experiment was carried out in batch with **Gel (3%)** and **Bead-BTZ** under direct sunlight
46 irradiation as an alternative to the 420 nm LED modules. All other parameters were kept the
47 same as described above for the batch reactions. The experimental set-up (Figure 6)
48 demonstrates the ease with which the experiment was carried out. Full conversion was observed
49
50
51
52
53
54
55
56
57
58
59
60

1
2
3 after 90 minutes with **Gel (3%)** and after 60 minutes with **Bead-BTZ** (Figure S29 and S30).
4
5 Under natural sunlight irradiation and aerobic conditions, along with comparable conversion
6 rates, we were able to validate the robustness of the synthesized photosensitizers. The ability to
7 use sunlight as a free source of energy and air as the source of oxygen demonstrates how two of
8 the main components for this photosensitization reaction greatly increase the potential for low
9 environmental impact applications.
10
11
12
13
14
15
16



33
34 **Figure 6.** Experimental set-up of the conversion of α -terpinene to ascaridole using $^1\text{O}_2$ produced
35 from direct sunlight irradiation.
36
37

38
39 **Aerobic oxidative hydroxylation of aryl boronic acids.** Due to the ability of the described
40 polymers to reach a stable excited triplet state for the generation of $^1\text{O}_2$, we successfully
41 demonstrated how these materials compare to our previous work.²⁷⁻²⁹ This prompted
42 investigations into the potential of these polymers to act as triplet photosensitizers in other
43 chemical transformations. Materials which can occupy an excited triplet state and subsequently
44 be employed as photocatalysts have been studied in depth and are well known.⁸ Within the
45 applications for which triplet photosensitizers can be employed, we envisaged the use of our
46 photoactive polymers for photoredox reactions.
47
48
49
50
51
52
53
54
55
56
57
58
59
60

1
2
3 One such reaction that has received much attention recently is the aerobic hydroxylation of
4 aryl boronic acids to phenols. Xiao *et al.* first reported the use of a visible-light photocatalytic
5 strategy to convert aryl boronic acids to phenols using Ru-based complexes and organic dyes.⁴²
6
7 The large scale synthesis of phenols is of great importance as they have wide applications in the
8 chemical and pharmaceutical industries. However, the photosensitizers employed for this process
9 are largely transition metal-based materials, which can be problematic when trace amounts of
10 these metals remain in the reaction products, as noted previously. More recently, Zhang *et al.*
11 reported the use of porous carbazole networks as effective visible-light heterogeneous
12 photocatalysts for organic synthesis, including the transformation of aryl boronic acids to
13 phenols.⁴³ This demonstrates the growing interest for metal-free, heterogeneous photocatalytic
14 materials. In this context, we implemented the synthesized polymers as heterogeneous
15 photosensitizers for the aerobic oxidative hydroxylation of aryl boronic acids.
16
17
18
19
20
21
22
23
24
25
26
27
28
29
30

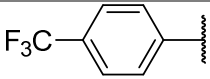
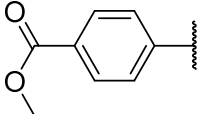
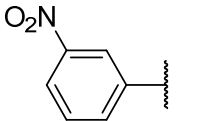
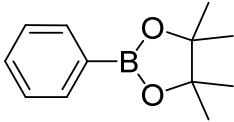
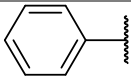
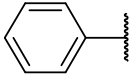
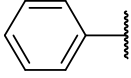
31 A standard model reaction was first performed for the oxidation of phenylboronic acid,
32 demonstrating full conversion *via* ¹H NMR spectroscopic analysis (see ESI) after 24 h. A series
33 of control experiments were then performed, eliminating either light, air, base or the
34 photocatalyst (Table S6). Each of these controls showed that no reaction occurred, indicating the
35 essential requirement of each component for this photocatalytic reaction. **St-BTZ** was employed
36 as a monomeric comparison to **Gel (5%)**. While photoactive, the monomer was unable to fully
37 convert phenylboronic acid to phenol within 24 h and was therefore less efficient. The focus of
38 this model reaction then turned to optimization of the reaction condition. Upon utilization of
39 different solvents (MeOH, CH₃CN) and bases (Et₃N, 1,8-diazabicyclo[5.4.0]undec-7-ene), we
40 discovered that the initial reaction conditions resulted in the swiftest time to full conversion of
41 the boronic acid.
42
43
44
45
46
47
48
49
50
51
52
53
54
55
56
57
58
59
60

1
2
3 A scope of reagents for aerobic oxidative hydroxylation of aryl boronic acids is summarized in
4 Table 1. Using the initial optimized reaction conditions, a range of substituted aryl boronic acids
5 were oxidized to the corresponding aryl alcohols until full conversion was demonstrated. A range
6 of electron-neutral, electron-donating and electron-withdrawing substituents were successfully
7 converted to the alcohols. We discovered that among these substrates, those with electron-
8 donating properties (Table 1, Entry 2-3) showed slower conversion rates (40-72 h) compared to
9 phenyl boronic acid. However, those with strong electron-withdrawing substituents (Table 1,
10 Entry 4-6) showed markedly increased conversion rate (18 h) when compared to the other
11 groups. One reagent that did not follow this trend was the ester-substituted phenyl boronic acid
12 (Table 1, Entry 5), showing full conversion after 48 h. Within this scope, we also extended the
13 use of these reaction conditions for the conversion of phenyl boronic pinacol ester, a derivative
14 of phenyl boronic acid, to phenol. To our surprise, full conversion to the phenol product was
15 seen after 15 h, nearly half the time required for the conversion of phenyl boronic acid (Table 1,
16 Entry 7).

17
18
19
20
21
22
23
24
25
26
27
28
29
30
31
32
33
34
35
36
37 **Table 1.** Light induced aerobic oxidative hydroxylation of aryl boronic acids.^a

Reaction scheme: $\text{HO-B(OH)}_2\text{-Ar} \xrightarrow[\text{DIPEA, 420 nm, DMF}]{\text{Photosensitizer}} \text{Ar-OH}$

Entry	Photosensitizer	Ar	Time (h)	Conversion (%) ^b
1	Gel (5%)		24	>99
2	Gel (5%)		72	>99
3	Gel (5%)		40	>99

4	Gel (5%)		18	>99
5	Gel (5%)		48	>99
6	Gel (5%)		18	>99
7	Gel (5%)		15	>99
8 ^c	pHIPE-BTZ		30	>99
9	Bead-BTZ (Batch)		10	>99
10 ^c	Bead-BTZ (Flow)		5	>99

^aReaction conditions: Aryl boronic acid (0.5 mmol/5 mL DMF), **Gel (5%)** (5 mg), DIPEA (1.0 mmol), DMF (5 mL), 420 nm LED irradiation, air, 24 h. ^bConversion calculated *via* ¹H NMR spectroscopy. DIPEA = *N,N'*-diisopropylethylamine, DMF = *N,N'*-dimethylformamide. ^cReaction performed under flow conditions.

Investigations into the mechanism of this reaction have been discussed within the literature and we believe the above reactions proceed in a similar fashion, through the generation of superoxide radicals *via* an electron transfer mechanism between the triplet photosensitizer and an amine base.^{42, 43} By removing the base and subsequent source of superoxide radicals, we have shown that ¹O₂, which we know is generated, has no effect on the aryl boronic acids. However, we have not found any experimental studies within the literature that investigate the generation of ¹O₂ along with O₂^{•-} in the presence of a base. To test this, α -terpinene, which is well known to react only with ¹O₂,³⁶ was added to the model reaction. The resultant ¹H NMR spectrum (Figure S45)

1
2
3 showed the presence of both the phenol and ascaridole products, confirming the concomitant
4 production $^1\text{O}_2$ and $\text{O}_2^{\cdot-}$ in the same reaction. While this may not have any particular benefit
5 regarding synthetic procedures, it is important to recognize as a potential issue when reactants or
6 products are particularly susceptible to an unwanted attack by $^1\text{O}_2$.
7
8
9

10
11
12 As a further showcase of the synthesized polymers as versatile heterogeneous triplet
13 photosensitizers, we implemented the optimized model reaction under flow conditions,
14 employing both **pHIPE-BTZ** and **Bead-BTZ**. The use of the immobilized **pHIPE-BTZ** resulted
15 in a time of 30 h to reach full conversion (Table 1, Entry 8). While this is a significantly longer
16 reaction time when compared to the model reaction in batch, we note that the total usage of the
17 photoactive polyHIPE at this point was around 80 h. During this time, the polyHIPE was
18 exposed to direct light irradiation, a variety of solvent and chemical systems and harsh oxidative
19 conditions. The fact that **pHIPE-BTZ** continued to display good photocatalytic activity after
20 such an extended and extreme use illustrates the robust and nearly indestructible nature of the
21 material. Implementation of **Bead-BTZ** under both batch and flow conditions was also
22 performed, both resulting in unsurprisingly accelerated conversion rates. Under batch conditions
23 the optimized model reaction required 10 h to show full conversion to the phenol product, more
24 than halving the time required when employing **Gel (5%)** as the photosensitizer. Under flow
25 conditions, the same reaction showed yet another dramatic decrease in reaction time with full
26 conversion occurring after only 5 h. When comparing these results to those of $^1\text{O}_2$ generation, a
27 large disparity can be seen with regards to the photoactive capabilities of the polymers under
28 different reaction conditions. While the gels and beads both showed comparable reaction rates
29 for $^1\text{O}_2$ generation, we now see a vast difference in effectiveness for the photoredox reaction.
30
31
32
33
34
35
36
37
38
39
40
41
42
43
44
45
46
47
48
49
50
51
52
53
54
55
56
57
58
59
60
This is most likely due to dissimilar physical characteristics between the two materials. While

1
2
3 the gels are able to swell greatly, they do not disperse as well as the beads in the same solvent
4 systems. The shape and size of **Bead-BTZ** aids in this as they form well distributed suspensions,
5
6 which can create a larger surface area by which triplet state interactions can occur. This idea can
7
8 also be applied to the decreased reaction time required for continuous flow over batch
9
10 conditions. A suspension can cause light penetration difficulties, resulting in areas of the reaction
11
12 mixture receiving lower flux and therefore a decrease in triplet state interactions. By applying the
13
14 same reaction in flow, we negated this issue as demonstrated by the change in the rate of
15
16 reaction.
17
18
19
20

21
22 Lastly, due to the enhanced capabilities of **Bead-BTZ**, we aimed to test both the reusability
23
24 and productivity of the beads under flow conditions using the same model reaction. We found
25
26 that beads showed good reusability, with full conversion occurring within the same time as the
27
28 first run (5 h) after six subsequent uses. Furthermore, and as explained previously, the **pHIPE-**
29
30 **BTZ** monolith was used over 30 times for the production of $^1\text{O}_2$ and then employed in the light
31
32 induced aerobic oxidative hydroxylation of aryl boronic acids, showing great photostability,
33
34 stability towards reactive oxygen species, and that it can be reused easily for both of the
35
36 reactions. The productivity of the material was investigated by determining the maximum
37
38 concentration that can be implemented where full conversion was still achieved after 5 h. From a
39
40 starting concentration of 0.1 mmol.mL^{-1} , we successfully increased this to 0.4 mmol.mL^{-1} before
41
42 longer reaction times were required. The dramatic reduction in reaction time, along with
43
44 reusability and productivity studies, further validates the use of continuous flow technology as a
45
46 tool for enhancing and optimizing reaction protocols even in heterogeneous photocatalysis.
47
48
49
50
51
52
53
54

55 CONCLUSION

56
57
58
59
60

1
2
3 A novel BTZ-based crosslinking monomer was synthesized and successfully copolymerized
4 with styrene to produce three insoluble polystyrene-based photosensitizers in different formats:
5 gels, beads and monoliths. These materials exhibited absorption wavelengths in the visible
6 spectrum (400-420 nm) and computational data suggested their ability to occupy the triplet
7 excited state. Thereafter, and as a proof of concept, the materials were employed successfully as
8 triplet photosensitizers in the production of $^1\text{O}_2$ and $\text{O}_2^{\cdot-}$ under different conditions. Whilst the
9 photoactive monomer demonstrated good photosensitizing properties, it was revealed to be
10 unstable in the presence of $^1\text{O}_2$. Through its incorporation into a polystyrene matrix, chemical
11 stability was improved dramatically without the loss of its photoactive properties and showed
12 better performance even at low concentrations. While the polymer gels proved to be efficient
13 triplet photosensitizers under batch conditions, they were not suitable for continuous flow
14 chemistry. Both **Bead-BTZ** and **pHIPE-BTZ**, designed for use under continuous flow
15 conditions, were shown to be exceptional photosensitizers. The polyHIPE in particular proved to
16 be an extremely stable and reusable photosensitizer, with total usage time exceeding 80 hours.
17
18
19
20
21
22
23
24
25
26
27
28
29
30
31
32
33
34
35

36 These materials have been reported as a proof of concept and through computational and
37 experimental methods, the polymer-supported monomer is clearly demonstrated as a robust
38 triplet photosensitizer. Currently, we are investigating the incorporation of other dyes into
39 polymeric systems through versatile free radical polymerization techniques, particularly within
40 water-compatible polymers for water and waste water treatment⁴⁴ and other systems requiring
41 biocompatibility. We acknowledge that photophysical studies are necessary to fully understand
42 the triplet excited state of these materials. However, the primary scope of this work aims to
43 describe the design and applications of a new class of materials. Whilst photophysical
44
45
46
47
48
49
50
51
52
53
54
55
56
57
58
59
60

1
2
3 characterization it is not a focus of the current work, it is an aspect we will look to address in the
4
5 future.
6
7
8
9

10 ASSOCIATED CONTENT

11
12
13 **Supporting Information.** Figures of commercial flow reactors; ^1H and ^{13}C NMR spectroscopic
14 data; Computational data; UV-Visible spectra; FT-IR spectra. This material is available free of
15 charge via the Internet at <http://pubs.acs.org>.
16
17
18
19
20

21 AUTHOR INFORMATION

22 Corresponding Author

23
24
25 * F. Vilela. Email: f.vilela@hw.ac.uk
26
27

28
29
30 * P. A. G. Cormack. Email: Peter.Cormack@strath.ac.uk
31
32
33

34 ACKNOWLEDGMENT

35
36
37 We would like to acknowledge Vapourtec Ltd. for their valuable technical support. F. Vilela
38 would like to thank Heriot-Watt University and The Royal Society for financial support
39 (RG140169). G. O. Lloyd would like to thank Heriot-Watt University and The Royal Society of
40 Edinburgh and Scottish Government for support through a RSE/SG Personal Research
41 Fellowship. M. J. Paterson would like to thank the EPSRC for funding through the platform
42 grant EP/P001459/1.
43
44
45
46
47
48
49
50
51

52 REFERENCES

53
54
55 (1) Xing, J.; Fang, W. Q.; Zhao, H. J.; Yang, H. G. *Chem. - Asian J.* **2012**, *7*, 642-657.
56
57
58
59
60

- 1
2
3 (2) Habisreutinger, S. N.; Schmidt-Mende, L.; Stolarczyk, J. K. *Angew. Chem., Int. Ed.* **2013**,
4
5 52, 7372-7408.
6
7
8
9 (3) Xuan, J.; Xiao, W.-J. *Angew. Chem., Int. Ed.* **2012**, 51, 6828-6838.
10
11
12 (4) Kruk, I. *Environmental Toxicology and Chemistry of Oxygen Species Handbook of*
13
14 *Environmental Chemistry*; Springer-Verlag: Berlin, 1998; pp 5-36.
15
16
17 (5) Schweitzer, C.; Schmidt, R. *Chem. Rev.* **2003**, 103, 1685-1757.
18
19
20 (6) Lamberts, J. J. M.; Neckers, D. C. *Tetrahedron* **1985**, 41, 2183-2190.
21
22
23 (7) DeRosa, M. C.; Crutchley, R. J. *Coord. Chem. Rev.* **2002**, 233-234, 351-371.
24
25
26 (8) Zhao, J.; Wu, W.; Sun, J.; Guo, S. *Chem. Soc. Rev.* **2013**, 42, 5323-5351.
27
28
29 (9) Kamkaew, A.; Lim, S. H.; Lee, H. B.; Kiew, L. V.; Chung, L. Y.; Burgess, K. *Chem. Soc.*
30
31 *Rev.* **2013**, 42, 77-88.
32
33
34 (10) Wu, W.; Guo, H.; Wu, W.; Ji, S.; Zhao, J. *J. Org. Chem.* **2011**, 76, 7056-7064.
35
36
37 (11) Wu, W.; Zhao, J.; Guo, H.; Sun, J.; Ji, S.; Wang, Z. *Chem. - Eur. J.* **2012**, 18, 1961-1968.
38
39
40 (12) Kopetzki, D.; Levesque, F.; Seeberger, P. H. *Chem. - Eur. J.* **2013**, 19, 5450-5456.
41
42
43 (13) Canonica, S.; Tratnyek, P. G. *Environ. Toxicol. Chem.* **2003**, 22, 1743-1754.
44
45
46 (14) Bonnett, R. *Chem. Soc. Rev.* **1995**, 24, 19-33.
47
48
49 (15) Awuah, S. G.; You, Y. *RSC Adv.* **2012**, 2, 11169-11183.
50
51
52 (16) Romero, N. A.; Nicewicz, D. A. *Chem. Rev.* **2016**, 116, 10075-10166.
53
54
55
56
57
58
59
60

- 1
2
3 (17) Punniyamurthy, T.; Velusamy, S.; Iqbal, J. *Chem. Rev.* **2005**, *105*, 2329-2364.
4
5
6 (18) Connick, W. B.; Gray, H. B. *J. Am. Chem. Soc.* **1997**, *119*, 11620-11627.
7
8
9 (19) Abdel-Shafi, A. A.; Beer, P. D.; Mortimer, R. J.; Wilkinson, F. *Phys. Chem. Chem. Phys.*
10 **2000**, *2*, 3137-3144.
11
12
13 (20) Abdel-Shafi, A. A.; Beer, P. D.; Mortimer, R. J.; Wilkinson, F. *J. Phys. Chem. A* **2000**,
14 *104*, 192-202.
15
16
17 (21) Goethals, A.; Mugadza, T.; Arslanoglu, Y.; Zügler, R.; Antunes, E.; Hulle, S. W.;
18 Nyokong, T.; Clerck, K. *J. Appl. Polym. Sci.* **2014**, *131*, 1-7.
19
20
21 (22) Kuznetsova, N. Sensitization of Singlet Oxygen Formation in Aqueous Media. In
22 *Photosensitizers in Medicine, Environment, and Security*; Nyokong, T. Ahsen, V., Eds.;
23 Springer: Netherlands, 2012; pp 267-314.
24
25
26 (23) Marin, M. L.; Santos-Juanes, L.; Arques, A.; Amat, A. M.; Miranda, M. A. *Chem. Rev.*
27 **2012**, *112*, 1710-1750.
28
29
30 (24) Guo, S.; Zhang, H.; Huang, L.; Guo, Z.; Xiong, G.; Zhao, J. *Chem. Commun.* **2013**, *49*,
31 8689-8691.
32
33
34 (25) Gerdes, R.; Bartels, O.; Schneider, G.; Wohrle, D.; Schulz-Ekloff, G. *Polym. Adv.*
35 *Technol.* **2001**, *12*, 152-160.
36
37
38 (26) Carpentier, R.; Leblanc, R. M.; Mimeault, M. *Enzyme Microb. Technol.* **1987**, *9*, 489-493.
39
40
41 (27) Zhang, K.; Kopetzki, D.; Seeberger, P. H.; Antonietti, M.; Vilela, F. *Angew. Chem., Int.*
42 *Ed.* **2013**, *52*, 1432-1436.
43
44
45
46
47
48
49
50
51
52
53
54
55
56
57
58
59
60

- 1
2
3 (28) Urakami, H.; Zhang, K.; Vilela, F. *Chem. Commun.* **2013**, *49*, 2353-2355.
4
5
6 (29) Zhang, K.; Vobecka, Z.; Tauer, K.; Antonietti, M.; Vilela, F. *Chem. Commun.* **2013**, *49*,
7 11158-11160.
8
9
10 (30) Tobin, J. M.; Liu, J.; Hayes, H.; Demleitner, M.; Ellis, D.; Arrighi, V.; Xu, Z.; Vilela, F.
11 *Polym. Chem.* **2016**, *7*, 6662-6670.
12
13
14 (31) Wong, Y. L.; Tobin, J. M.; Xu, Z.; Vilela, F. *J. Mat. Chem. A* **2016**, *4*, 18677-18686.
15
16
17 (32) Global Styrene Production - Merchant Research and Consulting Ltd.
18 [http://mcgroup.co.uk/news/20130830/global-styrene-production-exceeded-264-million-](http://mcgroup.co.uk/news/20130830/global-styrene-production-exceeded-264-million-tonnes.html)
19 [tonnes.html](http://mcgroup.co.uk/news/20130830/global-styrene-production-exceeded-264-million-tonnes.html) (accessed May 1, 2017).
20
21
22 (33) Cowie, J. M. G.; Arrighi, V. *Polymers: Chemistry and Physics of Modern Materials*, 3rd
23 *Ed.*; CRC Press: Florida, **2008**; pp 1-28, 57-97.
24
25
26 (34) *Gaussian 09*, Revision D.01; Gaussian, Inc.: Wallingford, CT, 2009.
27
28
29 (35) Geuskens, G.; David, K. In *The Photo-oxidation of Polymers. A Comparison with Low*
30 *Molecular Weight Compounds*, Plenary Lectures Presented at the Seventh Symposium on
31 Photochemistry, Leuven, Belgium, July 24-28, 1978; Reiser, A., Ed.; Elsevier: London, 1979.
32
33
34 (36) Schenck, G. O.; Ziegler, K. *Naturwissenschaften* **1944**, *32*, 157.
35
36
37 (37) Rabek, J. F. *Photodegradation of Polymers*; Springer-Verlag; Berlin, 1996; pp 51-97.
38
39
40 (38) Baumann, M.; Baxendale, I. R. *Beilstein J. Org. Chem.* **2013**, *9*, 1613-1619.
41
42
43 (39) Levesque, F.; Seeberger, P. H. *Angew. Chem., Int. Ed.* **2012**, *51*, 1706-1709.
44
45
46
47
48
49
50
51
52
53
54
55
56
57
58
59
60

1
2
3 (40) Centi, G.; Perathoner, S. Methods and Tools of Sustainable Industrial Chemistry: Process
4 Intensification. In *Sustainable Industrial Chemistry: Principles, Tools and Industrial Examples*;
5 Cavani, F., Centi, G., Perathoner, S., Trifiro, F., Eds.; Wiley-VCH Verlag GmbH & Co. KGaA:
6 Weinheim, Germany, 2009; pp 199-256.
7

8
9
10
11
12 (41) Rubio-Martinez, M.; Batten, M. P.; Polyzos, A.; Carey, K-C.; Mardel, J. I.; Lim, K-S.;
13 Hill, M. R. *Sci. Rep.* **2014**, *4*:5443, 1-5.
14
15

16
17
18 (42) Zou, Y.-Q.; Chen, J.-R.; Liu, X.-P.; Lu, L.-Q.; Davis, R. L.; Jorgensen, K. A.; Xiao, W.-J.
19
20
21
22
23
24
25
26
27
28
29
30
31
32
33
34
35
36
37
38
39
40
41
42
43
44
45
46
47
48
49
50
51
52
53
54
55
56
57
58
59
60

(43) Luo, J.; Zhang, X.; Zhang, J. *ACS Catal.* **2015**, *5*, 2250-2254.

(44) Shen, J.; Steinbach, R.; Tobin, J. M.; Mouro Nakata, M.; Bower, M.; McCoustra, M. R.
S.; Bridle, H.; Arrighi, V.; Vilela, F. *Appl. Catal., B* **2016**, *193*, 226-233.

1
2
3
4
5
6
7
8
9
10
11
12
13
14
15
16
17
18
19
20
21
22
23
24
25
26
27
28
29
30
31
32
33
34
35
36
37
38
39
40
41
42
43
44
45
46
47
48
49
50
51
52
53
54
55
56
57
58
59
60

For Table of Contents only.

